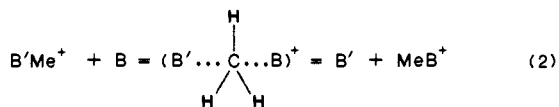# Methyl Cation Affinities

Terrance B. McMahon,[‡] Thomas Heinis,[†] Gordon Nicol,[†] Jamey K. Hovey,[‡] and Paul Kebarle*,[†]

Contribution from the Chemistry Departments, University of Alberta, Edmonton, Alberta, Canada T6G 2G2, and University of Waterloo, Waterloo, Ontario, Canada N2L 3G1. Received March 4, 1988

Abstract: Measurement of the CH_3^+ (Me^+) transfer equilibria, $B'Me^+ + B = B' + MeB^+$, with a pulsed high-pressure mass spectrometer and an ion cyclotron resonance mass spectrometer led to a scale of relative methyl cation affinities of bases B, MCA(B). This scale when calibrated to the literature value for the Me^+ affinity of N_2 led to absolute MCA values for the other 24 bases B that were part of the scale. Rate constants for several Me^+ transfer reactions were determined also. These were equal to collision rates for large exothermicity of the reactions and decreased below collision rates at low exothermicities. The MCA(B) values follow in general the proton affinities PA(B). A plot of PA(B) vs. MCA(B) leads to a slope of ~ 3 at low MCA(B) which becomes close to ~ 1 at high MCA(B). It is shown that this behavior can be rationalized.

This paper presents thermochemical data for the methyl cation (Me^+) affinities of bases B, MCA(B), which correspond to the enthalpy change ΔH°_1 for the dilute gas-phase reaction 1. The

$$BMe^+ = B + Me^+ \qquad (1)$$

$$B'Me^+ + B = (B' \ldots \overset{\overset{\textstyle H}{|}}{\underset{\diagup \, \diagdown}{C} \ldots B})^+ = B' + MeB^+ \qquad (2)$$
$$H \quad H$$

ΔH°_1 were obtained through determinations of the Me^+ transfer equilibria 2 which are cationic S_N2 reactions. The resulting, free energy changes, $\Delta G^\circ_2 = -RT \ln K_2$, could be converted to ΔH°_2 by estimates of the small ΔS°_2 changes. A scale of interconnected ΔG°_2 and also a scale of ΔH°_2 changes were obtained. The ΔH°_2 scale could be converted to a ΔH°_1 scale with use of available literature values of ΔH°_1 for one of the bases B. In this manner MCA(B) for some 25 bases B could be obtained.

The above methodology is analogous to that used for the determination of proton affinities via measurements of proton transfer equilibria.[1a] Proton transfer equilibria measurements have led to proton affinities of literally thousands of compounds.[1,2] On the other hand, previous MCA determinations have been very limited, yet methylation reactions like (2) are of importance in an extremely wide range of research areas. To indicate the scope, one may mention (a) $Me^+ \cdot B$ formation by the reverse of (1) in interstellar clouds where B may be Ne, H_2, O_2, CO, CO_2, etc., and the transfer of Me^+ to other B via bimolecular reactions (2) and its presumed significance to interstellar molecular synthesis;[3] (b) methylation and alkylation in organic synthesis undertaken in solution with use of diazonium ions,[4] MeN_2^+ and RN_2^+, or halonium ions,[5] $MeXR^+$; (c) carcinogenicity of alkylating agents, believed to achieve activity by conversion to highly reactive diazonium cations which alkylate nucleophilic sites in DNA.[6]

Although the present studies are for the gas-phase species, they can be of significance also for the understanding of the processes occurring in solution. The gas-phase thermochemical data relate directly to energy changes obtained by quantum chemical computation which provide essential complementary information on structures and energy.[6-8] Furthermore, comparison between the energy changes in the gas phase and solution can be expected to provide important insights into the solvent effects. Certainly this approach has proven most fruitful in the study of gas-phase and solution Brønsted acidities and basicities.[1]

The experimental gas-phase studies of MCA's were initiated by Beauchamp.[9] Significant development using both ICR and high-pressure mass spectrometric techniques has occurred since then and will be considered in the Discussion.

Experimental Section

Most of the measurements were made with a pulsed electron high-pressure mass spectrometer, PHPMS, which has been described.[10] The experimental conditions and procedures were similar to those used in earlier work.[1a] All measurements were performed at 400 K ion source temperature. At this elevated temperature the formation of ion clusters like Me^+B_2 etc. is much reduced and does not interfere with the equilibria measurements.

The gas mixture entering the ion source was passed through a cold trap located close to the ion source. This removed traces of water vapor. The temperature of the trap was varied from -77 to -160 °C depending on the volatility of the bases B used; i.e., the temperature was chosen to be high enough so as to pass through B but retain H_2O.

Some of the measurements were performed with an ion cyclotron resonance (ICR) spectrometer which has previously been described in detail.[11,12]

Results and Discussion

a. Typical Equilibria Measurements of Me^+ Transfer Reactions. Many of the Me^+ transfer equilibria were achieved by producing first the dimethylfluoronium ion, $CH_3FCH_3^+$, and using this ion as the primary reagent in the Me^+ transfer. The ion intensities observed in a PHPMS run used to elucidate the reaction sequence leading to $CH_3FCH_3^+$ are given in Figure 1. The major gas is nitrogen and electron impact ionization of N_2 leads to N_2^+ and N^+. In the absence of CH_3F, the N_2^+ is converted to N_4^+ and the N^+ to N_3^+, within ~ 50 μs, such that a distribution of N_4^+ to N_3^+ of 80:20 results.[13] In the present case (see Figure 1), because of the low CH_3F pressure the same conversion occurs almost to completion. Therefore, the ions reacting with CH_3F are predominantly N_4^+ and N_3^+ in an 80:20 ratio. Probably, the

(1) (a) McMahon, T. B.; Kebarle, P. *J. Am. Chem. Soc.* **1985**, *107*, 2612. (b) Taft, R. W. *Prog. Phys. Org. Chem.* **1983**, *14*, 248. (c) Brauman, J. I. *Annu. Rev. Phys. Chem.* **1983**, *34*, 187, and references therein.

(2) Lias, S. G.; Liebman, J. F.; Levin, R. *J. Phys. Chem. Ref. Data* **1984**, *13*, 695.

(3) (a) Adams, N. G.; Smith, D. *Chem. Phys. Lett.* **1981**, *79*, 563. (b) Smith, D.; Adams, N. G. *Astrophys. J.* **1978**, *L87*, 220.

(4) Keating, J. T.; Skell, P. S. In *Carbonium Ions*; Olah, G., Schleyer, P. v. R., Eds.; Wiley-Interscience: New York, 1970; Vol. II, Zollinger, H. *Azo and Diazo Chemistry*; Interscience: New York, 1961. Zollinger, H. *Acc. Chem. Res.* **1973**, *6*, 335. Krimze, w. *Angew. Chem., Int. Ed. Engl.* **1976**, *15*, 251.

(5) Olah, G. A. *Halonium Ions*; Wiley: New York, 1975.

(6) Ford, G. P.; Scribner, J. D. *J. Am. Chem. Soc.* **1983**, *105*, 349.

(7) Raghavachari, K.; Chandrasekhar, J.; Burnier, R. C. *J. Am. Chem. Soc.* **1984**, *106*, 3124.

(8) Vincent, M. A.; Radom, L. *J. Am. Chem. Soc.* **1978**, *100*, 3306.

(9) Holtz, D.; Beauchamp, J. L.; Woodgate, S. D. *J. Am. Chem. Soc.* **1970**, *92*, 7484.

(10) Kebarle, P. In *Techniques for the Study of Ion-Molecule Reactions* (*Techniques of Chemistry Series*); Saunders, W., Farrar, J. M., Eds.; Wiley-Interscience: New York, 1988.

(11) Hovey, J. K.; McMahon, T. B. *J. Am. Chem. Soc.* **1986**, *108*, 1719.

(12) Hovey, J. K.; McMahon, T. B. *J. Phys. Chem.* **1987**, *91*, 4560.

(13) Good, A.; Durden, D. A.; Kebarle, P. *J. Chem. Phys.* **1970**, *52*, 212.
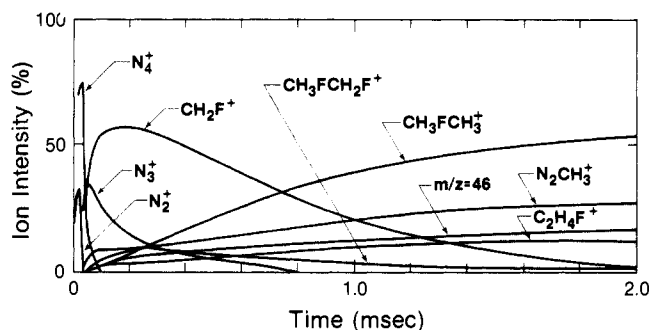
† University of Alberta.
‡ University of Waterloo.

7592 *J. Am. Chem. Soc., Vol. 110, No. 23, 1988*

McMahon et al.

Figure 1. Relative ion intensity time dependence after electron pulse. Gases in ion source: N_2, 3.5 Torr; CH_3F, 0.4 mTorr; T = 400 K. Reaction sequence eq 3–6 (see text) leads to major products $CH_3FCH_3^+$ and $CH_3N_2^+$.
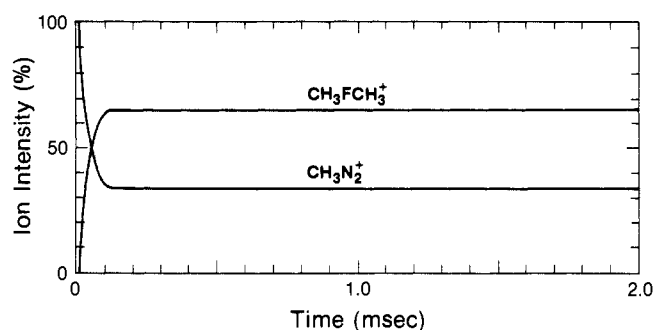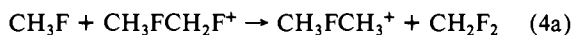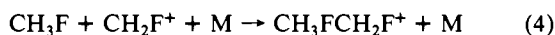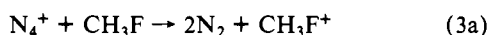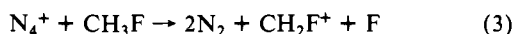

Figure 2. At a CH_3F pressure which is 10 times higher than that used in Figure 1, $CH_3FCH_3^+$ and $CH_3N_2^+$ reach equilibrium rapidly: N_2, 5 Torr; CH_3F, 5 mTorr.

dominant N_4^+ produces mostly CH_2F^+ ions by the dissociative charge transfer reaction (3); see Figure 1. The fluoromethyl cation

$$N_4^+ + CH_3F \rightarrow 2N_2 + CH_2F^+ + F \qquad (3)$$

$$N_4^+ + CH_3F \rightarrow 2N_2 + CH_3F^+ \qquad (3a)$$

$$CH_3F + CH_2F^+ + M \rightarrow CH_3FCH_2F^+ + M \qquad (4)$$

$$CH_3F + CH_3FCH_2F^+ \rightarrow CH_3FCH_3^+ + CH_2F_2 \qquad (4a)$$

$$CH_3FCH_3^+ + N_2 \rightleftarrows CH_3F + CH_3N_2^+ \qquad (5)$$

$$CH_3F^+ + CH_3F = CH_3FH^+ + CH_2F \qquad (6)$$

$$CH_3FH^+ + CH_3F = CH_3FCH_3^+ + HF \qquad (6a)$$

is known[14] not to undergo bimolecular reactions with CH_3F. In the present case, the slow disappearance of this cation should be due to the third body dependent association with CH_3F shown in (4). This reaction is followed by the nucleophilic displacement reaction (4a) which leads to the desired dimethylfluoronium ion. In the presence of the large excess of N_2, some endothermic Me^+ transfer occurs via (5), a reaction that is reversible but which has not yet reached equilibrium in Figure 1. When larger pressures of CH_3F are provided, the ions engaged in the reversible reaction (5) become dominant quite early and reach equilibrium much faster. This is illustrated in Figure 2. Runs under such concentration conditions were used to determine the equilibrium constant K_5.

Some CH_3F^+ is also produced by charge transfer from N_4^+; see reaction 3a. This ion could be observed when the CH_3F pressures were lower than that used in the run of Figure 1. The CH_3F^+ disappeared rapidly, presumably by the sequence of bimolecular reactions 6 and 6a which also lead to $CH_3FCH_3^+$. These reactions proceed at near Langevin collision rates; see Beauchamp[15] and Harrison.[16]
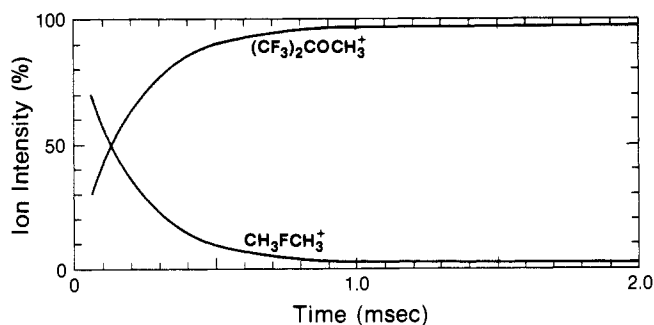
(14) Blint, R. J.; McMahon, T. B.; Beauchamp, J. L. *J. Am. Chem. Soc.* **1974**, *96*, 1269.

(15) Beauchamp, J. L.; Holtz, D.; Woodgate, S. D.; Patt, S. L. *J. Am. Chem. Soc.* **1972**, *94*, 2798.

Figure 3. Ion intensities observed with N_2 (3.5 Torr), CH_3F (33 mTorr), and $(CF_3)_2CO$ (11 mTorr); T = 400 K. The equilibrium $CH_3FCH_3^+$ + $OC(CF_3)_2 = CH_3F + CH_3OC(CF_3)_2^+$ is reached rather slowly even though $p(CF_3)_2CO$ is relatively high. This is due to a low rate constant of the reaction.
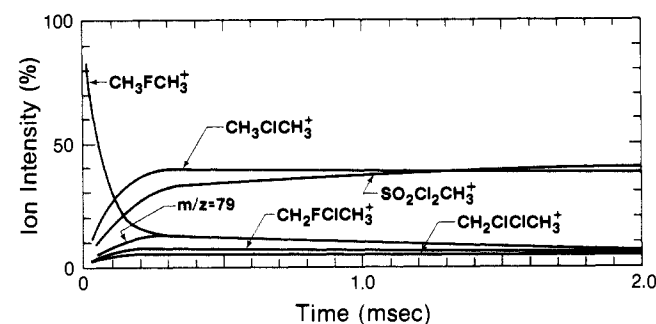

Figure 4. Example of a run where $CH_3FCH_3^+$, produced rapidly by reactions 3–6 (see Figure 1 and text), is used to transfer Me^+ to two bases, CH_3Cl and SO_2Cl_2, which then engage in Me^+ transfer equilibrium: N_2, 3.5 mTorr; CH_3F, 100 mTorr; CH_3Cl, 1 mTorr; SO_2Cl_2, 1.7 mTorr; 400 K.

Table I. Reproducibility of Equilibrium Constant K_2 for Different Concentrations of B′ and B[a]

$p(CH_3Cl)^b$	$p(SO_2Cl_2)^b$	K_2
5.3	1.7	1.1
4.4	1.4	0.8
1.2	4.0	1.1
0.8	2.7	1.6
1.2	9.9	1.6
1.2	12.6	0.8
1.0	10.7	1.2

[a] For reaction: $CH_3ClCH_3^+ + SO_2Cl_2 = CH_3Cl + SO_2Cl_2CH_3^+$, at 400 K. [b] Ion source pressures in mTorr.

The ion intensities shown in Figure 3 illustrate the measurement of an equilibrium between $CH_3FCH_3^+$ and a base B = perfluoroacetone, which has an MCA that is higher than that of CH_3F. The use of relatively high partial pressures for CH_3F leads to rapid production of the dimethylfluoronium ion. The equilibrium 7 is reached after ~ 1 ms (see Figure 3) even though the

$$CH_3FCH_3^+ + OC(CF_3)_3 = CH_3F + CH_3OC(CF_3)_2^+ \qquad (7)$$
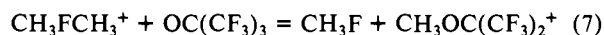
perfluoroacetone pressure is relatively high. This result indicates that the rate constant k_7 for the forward direction is considerably below the collision limit ($k_7 \approx 2 \times 10^{-11}$ molecule^{-1} cm^3 s^{-1}). It is shown in the kinetic section that this slow reaction is not an isolated case; i.e., a good fraction of the exothermic Me^+ transfer reactions proceed at rates which are considerably below collision rates. Slow Me^+ transfer rates make the equilibria measurements more difficult since other faster competitive reactions may change the concentrations of the ions engaged in the Me^+ transfer equilibrium.

In the above example CH_3F is one of the bases B engaged in the Me^+ transfer equilibrium. Many Me^+ equilibria were measured where CH_3F was not one of the bases engaged in the

(16) Herod, A. A.; Harrison, A. G.; McAskill, N. A. *Can. J. Chem.* **1971**, *49*, 2217.

Methyl Cation Affinities

J. Am. Chem. Soc., Vol. 110, No. 23, 1988 7593

ΔG°_2

ΔG°_{13}

13.9 CH$_3$B
1.1   0.1
12.9 SO$_2$Cl$_2$.
12.8 CH$_3$Cl
1.2   0.3   1.2   2.8 2.5
12.4 CS$_2$
(11.6) CF$_3$CN
1.8 2.0 3.0   3.5
11.4 SO$_2$
11.2 CF$_3$I
1.2
10.5 CF$_3$COCl
0.1
(10.3) PF$_3$
(10.0) CF$_3$COF
2.9   3.6
9.4 COS
9.3 (CF$_3$)$_2$CO
0.3   0.5
8.6 HBr
6.0 SO$_2$F$_2$
2.0 1.2   1.2 0.8 1.4   1.7   1.1 0.8
5.7 CH$_3$F
4.9 HCl
(4.9) N$_2$O
4.2
(4.6) Xe
5.7   6.0
(4.5) CF$_3$Br
(4.0) NF$_3$
3.9 CF$_3$Cl
(1.5) CO$_2$
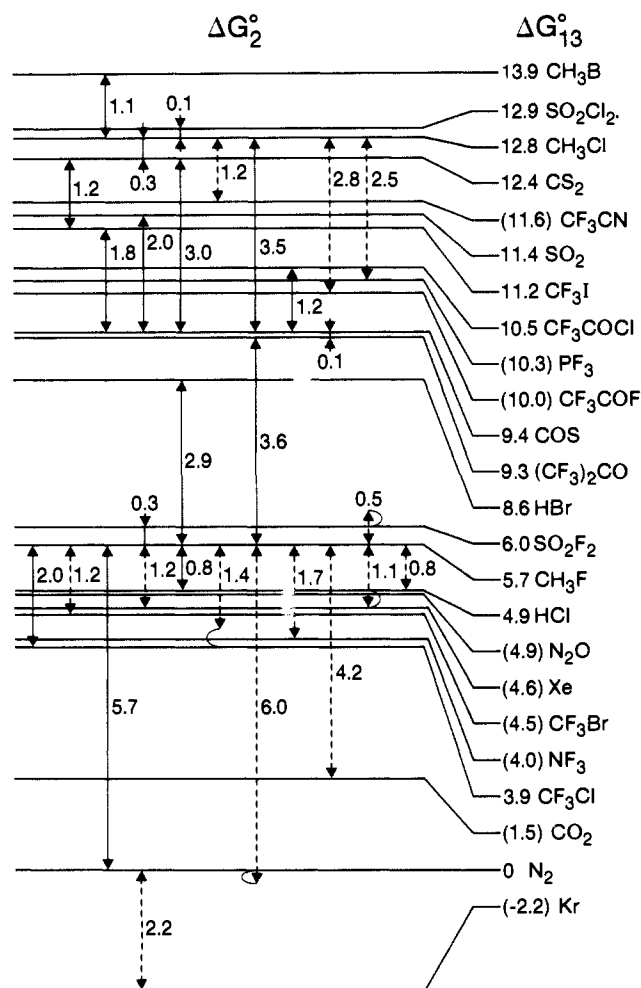0 N$_2$
2.2
(-2.2) Kr

Figure 5. Free energy changes ΔG°_2 from equilibrium constants K_2 for reactions 2: $B'CH_3^+ + B = B' + CH_3B^+$: solid arrows, PHPMS data at 400 K; dashed arrows, ICR results at 300 K. ΔG°_{13} values obtained from summation of ΔG°_2 correspond to free energy change for reaction 13: $N_2CH_3^+ + B = N_2 + CH_3B^+$.

equilibrium. Even in these experiments, very often CH$_3$FCH$_3^+$ was used as the primary methylating agent of the two bases of interest. This was done when both bases had MCA's which were considerably higher than that of CH$_3$F. Typically, the gas mixtures contained N$_2$ as major gas and relatively high pressures (50–100 mTorr) of CH$_3$F, while the two bases B were in the 1–5 mTorr range. Under these conditions reactions 1–6 produced rapidly CH$_3$FCH$_3^+$ which then transferred Me$^+$ to the two bases. An example of such a run is given in Figure 4 where the two MeB$^+$ at equilibrium are CH$_3$ClCH$_3^+$ and CH$_3$SO$_2$Cl$_2^+$.

In general the concentration of the bases was changed in separate runs and the resulting ion equilibria were measured. Table I illustrates the type of consistency obtained for equilibrium 8,

$$CH_3ClCH_3^+ + SO_2Cl_2 = CH_3Cl + CH_3SO_2Cl_2^+ \quad (8)$$
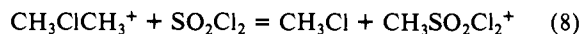
for which one run was displayed in Figure 4.

In general, the measurement of the Me$^+$ transfer equilibria was considerably more difficult than previous PHPMS proton transfer equilibria measurements. In the proton transfer measurements, conditions could be achieved where the two protonated species represented better than the 80% of the total ion concentration. Furthermore these equilibria almost always proceeded at collision rates in the exothermic direction. In the MCA equilibria, in addition of the two MeB$^+$ ions, often there were other ions produced by obscure reactions. Also, some of the Me$^+$ transfer reactions were slow. For these reasons we have assigned somewhat larger uncertainties to the MCA results. In the most unfavorable cases, relative errors in the ΔG°_2 measurements of ± 1 kcal/mol cannot be excluded.

4
CH$_3$FCH$_3$
CH$_3$ClCH$_3^+$
3
CH$_3$ClCH$_2$F$^+$
log (cpc)
2
CH$_2$F$^+$
CH$_3$N$_2^+$
1
0
(A)
0   0.5   1.0

100
CH$_2$F$^+$
Ion Intensity (%)
(B)
CH$_3$ClCH$_3^+$
50
CH$_3$ClCH$_2$F$^+$
CH$_3$N$_2^+$
CH$_3$FCH$_3^+$
0
0   0.5   1.0
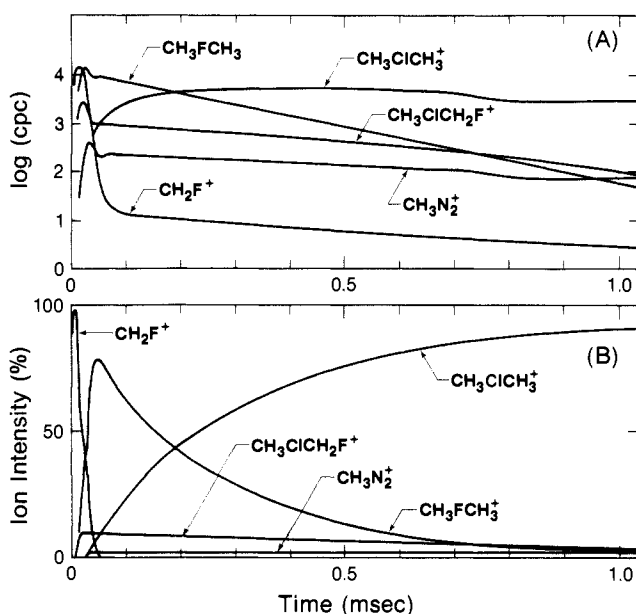Time (msec)

Figure 6. Ion intensity time dependence in a run used to determine rate constant k for the reaction CH$_3$FCH$_3^+$ + ClCH$_3$ = CH$_3$F + CH$_3$ClCH$_3^+$. (A) The logarithms of the measured ion intensities in counts per channel. The linear decrease of the CH$_3$FCH$_3^+$ ion is due to the pseudo-first-order Me$^+$ transfer reaction. (B) The corresponding relative intensities in a linear plot.

Equilibrium constants K_2 for the general Me$^+$ transfer reaction (2) determined by the measurements described above were used to obtain the corresponding ΔG°_2 values. The resulting ladder of interconnected ΔG°_2 values is shown in Figure 5. The PHPMS results are for 400 K while the ICR are for 300 K. Even though the temperatures are different, the ΔG°_2 can be compared directly since ΔS°_2 is generally small, which means that the temperature effect on the ΔG°_2 is small. In general, there is good agreement between the PHPMS and ICR results; see data for CF$_3$Cl (within 0.6 kcal/mol), HCl (within 0.4 kcal/mol), and SO$_2$F$_2$ (within 0.2 kcal/mol), and difference between N$_2$ and CH$_3$F (within 0.3 kcal/mol) (see Figure 5).

The thermochemical data based on the results in Figure 5 are discussed in sections c and d of the Results and Discussion.

b. Rate Constants for Me$^+$ Transfer Reactions from Me$_2$F$^+$ and Me$_2$Cl$^+$ to Bases B. The rate constants for several Me$^+$ transfer reactions from CH$_3$FCH$_3^+$ to different bases B were determined in a number of special experiments where the partial pressure of CH$_3$F was relatively high, such that formation of CH$_3$FCH$_3^+$ by reactions 3–6 was rapid, while the pressure of B was relatively low so that the kinetics of the CH$_3$B$^+$ production by CH$_3^+$ transfer from CH$_3$FCH$_3^+$ occurred within the time window of the PHPMS. The results from such a typical run are shown in Figure 6, which gives both a logarithmic plot of the absolute intensities and a linear plot of the relative ion concentrations. The logarithmic plot gives a good picture of low intensity ions that are also present, while the linear "normalized" plot provides a picture of the main events, i.e., reaction 9. A plot of

$$CH_3FCH_3^+ + ClCH_3 \rightarrow CH_3F + CH_3ClCH_3^+ \quad (9)$$
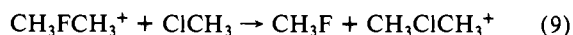
the natural logarithm of the normalized intensity of CH$_3$FCH$_3^+$ vs. time gave a straight line whose slope is identified with ν_9, the pseudo-first-order rate constant. The known concentration of B = CH$_3$Cl was then used to obtain k_9, see eq 10.

$$\nu = k[B] \quad (10)$$

Determinations of ν at different [B] gave invariant rate constants k for this and the other reactions studied. The results of the kinetic determinations are summarized in Table II. Included in the table are also results from previous determinations[17] of the

(17) Sen Sharma, D. K.; Kebarle, P. *J. Am. Chem. Soc.* **1982**, *104*, 19.

7594 *J. Am. Chem. Soc., Vol. 110, No. 23, 1988*

McMahon et al.

Table II. Rate Constants k for Reactions: $Me_2X^+ + B = MeX + MeB^+$

X	B	$(k \times 10^9)^c$	$(-\Delta G^\circ)^d$
F^a	CH_3Cl	1.4	7.1
	CS_2	1.4	6.4
	SO_2Cl_2	1.0	7.2
	SO_2	0.3	5.7
	SO_2ClF	0.3	$\sim 5.7^e$
	$(CF_3)_2CO$	0.02	3.6
Cl^b	$(CH_3)_3N$	1.2	64
	H_3N	0.8	43
	$(CH_3)_2O$	1.1 $(0.5)^f$	31
	C_2H_5OH	0.5	27
	$CH_3C_6H_5$	0.05	34
	C_6H_6	0.002	33

^{a}Temperature 400 K, present work. ^{b}Temperature 315 K, from Sen Sharma.[17] ^{c}In molecule^{-1} cm^3 s^{-1}. ^{d}Free energy change of reaction in kcal/mol ($\Delta G^\circ \approx \Delta H^\circ$): for F from Figure 5 and Table III; for Cl from Sen Sharma.[17] ^{e}Estimate based on assumption that ΔG° for SO_2ClF should be between SO_2Cl_2 and SO_2F_2 but closer to SO_2Cl_2; see Figure 5. ^{f}Value for 400 K from Sen Sharma.[17]
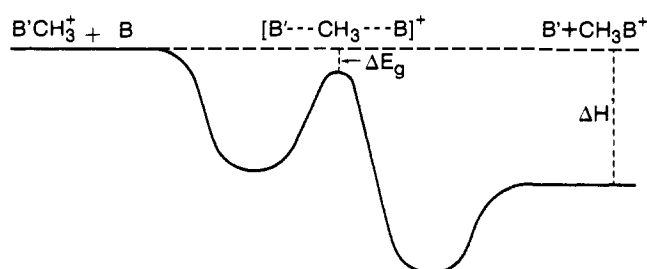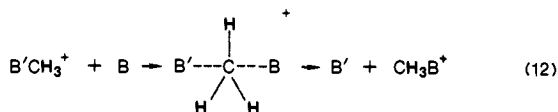

Figure 7. Gas-phase reaction coordinate for cationic S_N2 reactions 2 involving Me^+ transfer. The energy difference between the intermediate $B'CH_3B^+$ and the reactants $B'CH_3^+$ and B, called ΔE_g, controls the rate. A large $-\Delta E_g$ leads to collision rates; a small $-\Delta E_g$ leads to negative temperature dependence and low rates.

rate constants involving Me^+ transfer from dimethylchloronium ion to bases B; see eq 11. Examining first the Me_2F^+ data in

$$CH_3ClCH_3^+ + B = CH_3Cl + CH_3B^+ \qquad (11)$$
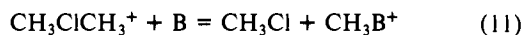
the table, we notice that the rate constants are close to the Langevin–ADO collision limit at higher exoergicities of the reaction and gradually decrease to considerably below the collision limit. Thus for B = perfluoroacetone at an exoergicity of 3.6 kcal/mol, the collision limit is higher by a factor of ~ 100 than the observed rate. A similar trend is observed for the Me_2Cl^+ data; however, in this case, the decrease occurs already at much higher exoergicities. It is most likely that the Me^+ transfer reactions 11 and 12 proceed by an S_N2 mechanism involving

$$B'CH_3^+ + B \rightarrow B'\text{---}\overset{\overset{\displaystyle H}{\displaystyle |}}{\underset{\overset{\displaystyle |}{\displaystyle H}\diagdown H}{C}}\text{---}B \rightarrow B' + CH_3B^+ \qquad (12)$$

"backside attack" and inversion of the methyl group.

A double minimum potential well is expected[17-19] for the reaction coordinate in the gas phase as shown in Figure 7. Theoretical calculations also have provided such double minima reaction coordinates; see Chandrasekhar[7] for Me^+ transfer from $MeOH_2^+$ to OH_2 and to CH_3OH. When the gap $(-\Delta E_g)$ is large (see Figure 7), the reactions proceed at collision rates. For reactions where the gap is small, the rate is slow and decreases as the temperature is increased (negative temperature dependence);[17] see, for example, data for Me_2Cl^+ and B = Me_2O in Table II.

(18) (a) Farneth, W. E.; Brauman, J. I. *J. Am. Chem. Soc.* **1976**, *98*, 7891. (b) Olmstead, W. N.; Brauman, J. I. *Ibid.* **1977**, *99*, 4219. (c) Asubiojo, O. I.; Brauman, J. I. *Ibid.* **1979**, *101*, 3715. Pellerite, M. J.; Brauman, J. I. *Ibid.* **1980**, *102*, 5993.

(19) Caldwell, G.; Magnera, T. F.; Kebarle, P. *J. Am. Chem. Soc.* **1984**, *106*, 959.
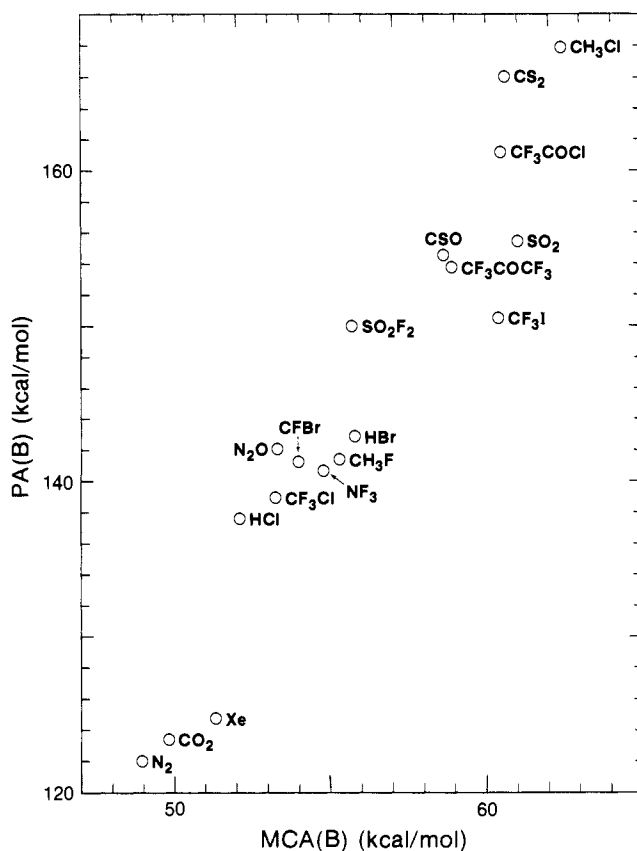

Figure 8. Plot of proton affinities PA(B) versus methyl cation affinities MCA(B) for bases of Table III; slope $\approx$ 3.

For the series of bases below B = Me_2O, the gap gradually gets smaller, and for benzene, the gap disappears; i.e., ΔE_g has become positive and the rate is very low and is found to increase with temperature.[17]

Neglecting entropic factors, a direct relationship between rate and gap width can be expected. The gap width is expected to increase monotonically with increase of reaction exoergicity and thus with the MCA(B) only when a series of related bases B is involved.[20] For example, the bases EtOH to Me_3N (see Me_2Cl^+ results in Table II) represent such a group (oxygen and nitrogen bases). The bases toluene and benzene fall in another group (carbon bases) which is much less nucleophilic. Substantial reaction exothermicity still occurs for the latter group owing to resonance stabilization (charge delocalization) present in the products but not in the transition state.[17] This means that the rates for this group are expected to be lower at equal exothermicity, relative to the first group.

The observed decrease of rates for Me^+ transfer from Me_2F^+ to B with decreasing exoergicity of the reactions, i.e., decreasing MCA(B) (Table II), is thus expected. Even though the nucleophilic centers on the bases involved are fairly dissimilar, still these are systems in which selective resonance stabilization of the products only does not occur to any extent. The experimental observation that for Me_2F^+ the rates remain close to collision rates down to very low exothermicities, while for Me_2Cl^2 they begin to decrease already at 30 kcal/mol exothermicities (B = Me_2O), cannot be attributed to different nucleophilicities of the bases used in the two groups. Thus Me_2O is more nucleophilic than all of the bases of the Me_2F^+ group. Obviously the difference must be due to differences between Me_2F^+ and Me_2Cl^+; i.e., reactions of Me_2F^+ would lead to a much larger gap $(-\Delta E_g)$ relative to reactions with Me_2Cl^+ when the same base B is involved. The observed greater reactivity of Me_2F^+ relative to Me_2Cl^+ is in line with the lower MCA of MeF relative to the MCA of MeCl; see

(20) Magnoli, D. E.; Murdoch, J. R. *J. Am. Chem. Soc.* **1981**, *103*, 7465. Dodd, J. A.; Brauman, J. I. *J. Phys. Chem.* **1986**, *90*, 3559.

Table III. Methyl Cation Affinities

B	$S°(B)^a$	$S°(CH_3{}^+B)^c$		$\Delta S°_{13}$	$\Delta G°_{13}{}^l$	$\Delta H_{13}{}^m$	$\Delta H(Me^+-B)^n$
CH₃Br				-2.6^f	14.1	14.9	63.3
SO₂Cl₂				-2^h	13.1	13.7	62.1
CH₃Cl	56.0			-2.1^f	13.0	13.6	62.0 $(64)^j$
CS₂	56.8			1.6	12.3	11.8	60.2
SO₂	59.3			-2^h	11.6	12.2	60.6
CF₃I				-1.3^e	11.3	11.6	60.0
CF₃COCl				-2^h	10.7	11.7	60.1
OCS	55.3	CH₃NCS	69.3^d	1.6	9.3	8.8	57.2
CF₃COCF₃				-2^h	9.5	10.1	58.5
HBr	47.5			4.4^g	8.2	7.0	55.4 $(59.8 \pm 3)^k$
SO₂F₂	67.7			-2^h	6.3	6.9	55.3
CH₃F	53.3	CH₃OCH₃	63.7	-2.0	5.9	6.5	54.9
HCl	44.6	CH₃SH	61.0^d	4.0	4.7	3.3	51.7 $(51 \pm 6)^k$
N₂O	52.5	CH₃NCO	65.1^b	0.2	5.1	4.5	52.9
Xe	40.5	CH₃I	60.7^d	7.8	4.8	2.5	50.9
CF₃Br	73.4^b			-1.3^e	4.7	5.2	53.6
NF₃	62.3	CH₃CF₃	68.7^b	-6.0	4.2	6.0	53.6
CF₃Cl	69.0^b	CF₃SCH₃	80.3^b	-1.1	4.2	4.5	52.9
CO₂	51.1	CH₃NCO	65.1^b	1.6	1.5	1.0	49.4
N₂	45.8	CH₃CN	58.1^d	0	0	0	$(48.4)^i$
Kr	39.2	CH₃Br	58.8^d	7.2	-2.2	-4.4	44.0

^{a} Entropies at 298 K in cal mol⁻¹ K⁻¹ from Benson[25] except where otherwise indicated: $\Delta G°_{13}$ at 300 K, $\Delta H°_{13}$, MCA(B), all in kcal/mol. ^{b} Estimates using group equivalents, Benson.[25] ^{c} Estimated entropy of CH₃B⁺ based on entropy for isoelectronic neutral shown. Values for isoelectronic neutrals from Benson[25] except where otherwise indicated. ^{d} From Stull et al.[26] ^{e} Assumed the same as $\Delta S°_{13}$ for reaction 13 involving CH₃Cl. ^{f} Assumed the same as $\Delta S°_{13}$ for reaction 13 involving CH₃F. ^{g} Assumed the same as $\Delta S°_{13}$ for HCl. ^{h} Arbitrary estimate. ^{i} External standard, Beauchamp et al.,[22] and $\Delta H°_f(CH_3N_2CH_3) = 35.5$ kcal/mol, Rossini.[22b] ^{j} Sen Sharma.[27] ^{k} Estimates based on bracketing literature data leading to PA(CH₃Cl) ≈ 158 ± 6 kcal/mol and PA(CH₃Br) ≈ 164.5 ± 3 kcal/mol; see text. ^{l} Estimated error ±0.5 kcal/mol. ^{m} Estimated error ±1 kcal/mol. ^{n} Estimated error ±3 kcal/mol.

Table IV. MCA(RCl)^a

Me	Et	i-Pr	t-Bu	eq 17
62.0^b	71^c	77^c	81^c	experimental
64.0	72	79	85	(MINDO/3)[27,28]

^{a} All values in kcal/mol. ^{b} Experimental result, present work, Table III. ^{c} Experimental results, Sen Sharma.[27]

Figure 5 and Table III. The generalization that for similar **B** the reactivity of MeB⁺ in electrophilic Me⁺ transfer reactions increases with decreasing MCA(B) may be expected to hold. In summary, the present kinetic results for the Me⁺ transfer reaction (12) are consistent with the assumption that $-\Delta E_g$ (see Figure 8) and thus the rates, when they are limited by the passage over the barrier, increase with increasing MCA of B and decreasing MCA of B'. The relationship is expected to hold well when series of related B and B' are involved. Such a series of related B' would be CH₃X where X = F, Cl, Br, I.

It is notable that these simple relationships, which are easily spotted in the gas phase where the complicating effect of the solvent is absent, can be experimentally demonstrated only when gas-phase ion–molecule reactions with rates lower than collision rates are encountered. Furthermore, in such cases the magnitude of the ΔE_g can often be determined.[18,19] Knowledge of the values of ΔE_g allows for the evaluation, via a Born cycle, of the solvation energy of the transition state for the corresponding reaction in solution.[21] This amounts to establishing a quantitative relationships between the reaction in the gas phase and solution.[21]

c. Thermochemical Data on Me⁺ Affinities. The $\Delta G°_2$ results for the Me⁺ transfer equilibria (2), Figure 5, can be combined to provide a scale giving the $\Delta G°_{13}$ value for the transfer reaction 13. The resulting values for $\Delta G°_{13}$ are given in Figure 5. N₂

$$N_2CH_3{}^+ + B = N_2 + CH_3B^+ \qquad (13)$$
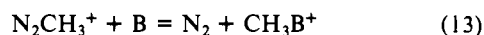
is the only base for which a good literature value for the MCA is available, and therefore this compound is used as the anchor point (primary standard) of the scale. Beauchamp et al.[22] have

measured the photoionization appearance potential of CH₃N₂⁺ from CH₃N₂CH₃. Combining their value with the latest $\Delta H_f°(CH_3N_2CH_3) = 35.5 \pm 1$ kcal/mol, due to Rossini,[22b] one obtains the heat of formation, $\Delta H°_f(CH_3N_2{}^+) = 212.9$ kcal mol⁻¹. From this value and $\Delta H_f(CH_3{}^+) = 261.2$ kcal/mol,[23] one obtains the MCA(N₂) = 48.3 kcal/mol; see eq 14. This MCA is used

$$N_2CH_3{}^+ = N_2 + CH_3{}^+ \qquad \Delta H°_{14} = MCA(N_2) =$$
$$48.3 \ kcal/mol^{22} \qquad (14)$$
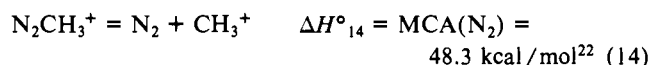
in Table III to construct an absolute MCA scale in combination with the results for $\Delta G°_{13}$ from Figure 5. Unfortunately photoionization appearance potentials do not always provide reliable ionic heats of formation so that $\Delta H°_{14}$ could be in error by a few kcal/mol.

Theoretical calculations[24] have established that CH₃N₂⁺ is linear. Unfortunately the MCA(N₂) provided by these calculations differ widely depending on the basis set used. Thus, Radom[24a] obtains with STO-3G, 51.6 kcal/mol, in fair agreement with the Beauchamp[22] result, but only 28.5 kcal/mol at the 4-31G level. Simonetta et al.,[24b] using a more flexible basis set which includes polarization functions, obtained the even lower value of 18.4 kcal/mol (for MNDO data, see Ford and Scribner[6]). Obviously, further extended basis set calculations including electron correlation and complete geometry optimization are very desirable.

In order to combine $\Delta H°_{14}$ with the free energy scale $\Delta G°_{13}$ of Figure 5, the $\Delta G°_{13}$ values for the Me⁺ transfer must be converted to $\Delta H°_{13}$ values. On principle, the $\Delta S°_{13}$ and $\Delta H°_{13}$ could have been obtained by measuring the temperature dependence of the Me⁺ transfer equilibria (2) and deriving $\Delta H°_2$ and $\Delta S°_2$ from van't Hoff plots. However, since the equilibria 2 were difficult to measure even at one single temperature, this method was not adopted, and instead the $\Delta S°_{13}$ values were estimated. The S°(B)'s for most B's available in the literature.[25,26] In a few

(21) Magnera, T. F.; Caldwell, G.; Sunner, J.; Ikuta, S.; Kebarle, P. *J. Am. Chem. Soc.* **1984**, *106*, 6140.

(22) (a) Foster, M. S.; Williamson, A. D.; Beauchamp, J. L. *Int. J. Mass Spectrom. Ion Phys.* **1974**, *15*, 429. (b) Rossini, F. D.; Montgomery, R. L. *J. Chem. Thermodyn.* **1978**, *10*, 465.

(23) Traeger, J. C.; McMoughlin, R. G. *J. Am. Chem. Soc.* **1981**, *103*, 3647.

(24) (a) Vincent, M. A.; Radom, L. *J. Am. Chem. Soc.* **1978**, *100*, 3306. (b) Demontis, P.; Ercoli, R.; Gamba, A.; Suffritti, G. B.; Simonetta, M. *J. Chem. Soc., Perkin Trans. 2* **1981**, 488.

(25) Benson, S. W. *Thermochemical Kinetics*, 2nd ed.; Wiley: New York, 1976.

(26) Stull. D. R.; Westrum, E. F., Jr.; Sinke, G. C. *The Chemical Thermodynamics of Organic Compounds*; Wiley: New York, 1969.

7596   *J. Am. Chem. Soc., Vol. 110, No. 23, 1988*

McMahon et al.

cases $S°(B)$ had to be estimated with the group equivalents method.[25] All the $S°(B)$ data used are given in Table III. $S°(CH_3B^+)$ values were assumed to be the same as those of the isoelectronic neutral. For example, $S°(CH_3N_2^+)$ was assumed to be equal to $S°(CH_3CN)$. $S°(CH_3B^+)$'s and the isoelectronic neutrals used are also given in Table III. $\Delta S°_{13}$ was then calculated from the $S°$ values of the reactants and products. In cases where the $S°$ values of the isoelectronic neutrals were not available, the $\Delta S°_{13}$'s were obtained by assuming that they are identical for homologous pairs. Thus $\Delta S°_{13}$ values for the reactions 15 were

$$N_2CH_3^+ + XCH_3 = N_2 + CH_3XCH_3^+ \quad (X = F, Cl, Br) \quad (15)$$
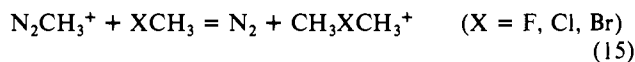
assumed to be identical. The $\Delta S°_{13}$'s evaluated in this manner were used to obtain $T\Delta S°_{13}$ for $T = 400$ K, and these combined with the PHPMS $\Delta G°_{13}$ led to a $\Delta H°_{13}$ scale. Evaluated $\Delta S°_2$ together with the ICR $\Delta G°_2$ were used to obtain $\Delta H°_2$ values for the compounds determined by ICR; these were then incorporated into the $\Delta H°_{13}$ scale via a common base B in reactions (2) used in PHPMS and ICR determinations. The $\Delta H°_{13}$ scale was then calibrated to the $\Delta H°_1(N_2) = MCA(N_2) = 48.3$ kcal/mol[22] and a $\Delta H_1(B) = MCA(B)$ scale was obtained.

The MCA(B) scale can be checked with available literature data at three points. The $MCA(CH_3Cl) = 63$ kcal/mol based on Sen Sharma et al.[27] and McManus[28] is close to the present value of 61.9 kcal/mol, Table III. Sen Sharma and McManus obtained MCA values from MINDO/3 calculations. The calculations by themselves would not have been convincing; however, Sen Sharma et al.,[27] on the basis of determinations of the temperature dependence of equilibria 16, obtained via van't Hoff plots $\Delta H°_{16}$

$$R^+ + ClCH_3 = RClCH_3^+ \quad (R = Et, i\text{-Pr}, t\text{-Bu}) \quad (16)$$

and from these and thermochemistry data, deduced the experimental MCA(RCl) given in Table IV. The relatively good agreement and consistent trends between the experimental MCA results[27] for RCl = EtCl, i-PrCl, t-BuCl and the MINDO/3 predicted values[27,28] suggests that the MINDO/3 result for the MCA(CH$_3$Cl) is too high by ~1 kcal/mol. The experimental and MINDO/3 correlation thus indicates an MCA (CH$_3$Cl) = 63 ± 2 kcal/mol.

Relationship 17, between the proton affinity of the methyl halide

$$PA(CH_3X) - MCA(HX) = \Delta H_f(H^+) - \Delta H_f(CH_3^+) +$$
$$\Delta H_f(CH_3X) - \Delta H_f(HX) = 104.5 + \Delta H_f(CH_3X) - \Delta H_f(HX) \quad (17)$$
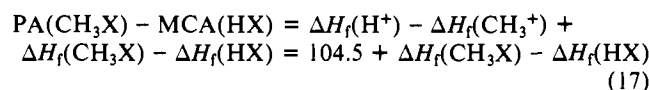
CH$_3$X and the Me$^+$ affinity of the corresponding hydrogen halide HX, follows from the definition of the PA and MCA. The value 104.5 kcal/mol for the difference is based on $\Delta H_f(H^+) = 365.7$ kcal/mol and $\Delta H_f(CH_3^+) = 261.2$ kcal/mol.[23]

The proton affinity of CH$_3$Cl has been established by Beauchamp et al.[15] to be between PA(C$_2$H$_4$) and PA(C$_2$H$_2$). Using the PA values 162.6 and 153.3 kcal/mol, respectively (Lias[2]), one estimates PA(CH$_3$Cl) ≈ 158 ± 6 kcal/mol which combined with $\Delta H_f(CH_3Cl) = -19.3$ kcal/mol,[29,30] $\Delta H_f(HCl) = -22.1$ kcal/mol,[31] leads via (17) to MCA(HCl) = 51 ± 6 kcal/mol. This can be compared with the present experimental value of 51.7 kcal/mol in Table III.

The proton affinity of CH$_3$Br has been bracketed[1a] between PA(C$_2$H$_4$) = 162.6 kcal/mol[2] and PA(H$_2$O) = 166.4 kcal/mol,[2] allowing an assignment of PA(CH$_3$Br) ≈ 164.5 ± 3 kcal/mol. This value combined with $\Delta H_f(CH_3Br) = -8.5$ kcal/mol,[30] $\Delta H_f(HBr) = -8.7$ kcal/mol,[31] leads to MCA(HBr) = 59.8 ± 3

(27) Sen Sharma, D. K.; De Hojer, S. M.; Kebarle, P. *J. Am. Chem. Soc.* **1985**, *107*, 3757.

(28) McManus, S. P. *J. Org. Chem.* **1982**, *47*, 3070.

(29) Pedley, J. B.; Naylor, R. D.; Kirby, S. P. *Thermochemical Data of Organic Compounds*, 2nd ed.; Chapman and Hall: London, 1986.

(30) Wagman, D. D., et al. *Selected Values of Chemical and Thermodynamic Properties (Technical Note 270-3)*; National Bureau of Standards: Washington, D.C., 1968.

(31) McMahon, T. B.; Kebarle, P. *Can. J. Chem.* **1985**, *63*, 3160.

Figure 9. Plot of PA(B) vs. MCA(B) including bases B from Figure 8 and bases XH whose MCA(XH) can be evaluated from PA(CH$_3$X) (see eq 17). Slope changes from ≈3 at low MCA(B) to ≈1 at high MCA(B): (O) bases from Table III, (●) bases XH.

kcal/mol, which can be compared with the present result (Table III) of 55.4 kcal/mol.

The above three comparisons with approximate MCA data from the literature are in support of the MCA ladder Table III and suggest an error in the absolute values of approximately ±3 kcal/mol.

Since in Table III MCA(HCl) and MCA(HBr) can be considered more accurate than the bracketed PA(CH$_3$Cl) and PA(CH$_3$Br), one can use eq 17 to determine PA values from the MCA. One obtains PA(CH$_3$Cl) = 159.0 kcal/mol and PA(CH$_3$Br) = 160.1 kcal/mol (see also McMahon[31]).

The present MCA scale, Table III, extends to MCA ≈ 63 kcal/mol. This is a value somewhat below but close to where the MCA's for oxygen bases like the ethers begin. Thus, from the known heat of formation of protonated dimethyl ether, ΔH_f ((CH$_3$)$_2$OH$^+$) = 130 kcal/mol,[2] one can evaluate the MCA(CH$_3$OH) = 83.2 kcal/mol. Therefore, the availability of the present scale holds the promise that future Me$^+$ transfer equilibria measurements to bases with MCA in the 70–80 kcal/mol range will lead to a link up to the numerous conventional oxygen bases and these in turn to the nitrogen bases. Thus, a complete scale of MCA based on equilibria covering a similar range to that available for the PA's[1,2] is made more likely by the availability of the present results.

d. Relationships between Proton and Methyl Cation Affinities. Only an approximate relationship between PA(B) and MCA(B) can be expected. When H$^+$ and CH$_3^+$ react with the same basic atom on B, the reaction is formally very similar since it consists of an electron pair donation from B to H$^+$ and CH$_3^+$. The PA(B) should be much larger than the MCA(B) for two reasons. First, the B–H bond formed will be stronger than the B–CH$_3$ bond; second, the electrostatic energy decrease due to the positive charge expansion from the very small H$^+$ to BH$^+$ will be very much larger than that for the expansion from the much bigger CH$_3^+$ to CH$_3$B$^+$. A more quantitative expression for these factors will be given below.

A plot of PA(B), from Lias,[2] versus the MCA(B) determined in the present work is shown in Figure 8. A fair straight line correlation with a slope ρ ≈ 3 is observed. In order to examine

the relationship over a wider range of data, MCA values for bases of the type HX where X now stands for a basic group like OH, OCH_3, etc., were evaluated from thermochemical data[2] with use of eq 17. The extended set is shown in the PA versus MCA plot, Figure 9. It is seen that the bases HX, where they overlap with the data for the general set of bases B, do blend in, i.e., do not form a noticeably distinct line.

The PA versus MCA relationship with the wider range of data, Figure 9, is not a straight line any more. The slope is seen to decrease from $\rho \approx 3$ (low MCA) to $\rho \approx 1$ (high MCA).

Equation 18 can be derived from eq 17 as shown below. The equation is exact only for bases HX; however, a certain interpretative meaning will be obtained from the equation, which is useful also for the general group B. Substitution of the definitions

$$PA(HX) - MCA(HX) =$$
$$IE(H) - IE(CH_3) + BE(H-X) - BE(CH_3-X) - \Delta PA(CH_3)$$
$$(18)$$

for the ionization energies (IE, eq 19), bond dissociation energies (BE, eq 20), and eq 21, which expresses the methyl substituent effect on the proton affinity of HX, into eq 17 leads directly to (18).

$$IE(H) = \Delta H_f(H^+) - \Delta H_f(H) \qquad (19)$$

$$BE(H-X) = \Delta H_f(H) + \Delta H_f(X) - \Delta H_f(HX) \qquad (20)$$

$$\Delta PA(CH_3) = PA(CH_3X) - PA(HX) \qquad (21)$$

Equation 18 can be given the following qualitative interpretation. As the base is protonated, a charge transfer occurs from H^+ to the base (measured by IE(H)) and a bond is formed (measured by BE(H–X)). The analogous terms $IE(CH_3)$ and $BE(CH_3-X)$ occur for CH_3^+ addition to the base. However, the charge transfer from H^+ (or CH_3^+) to the base is not complete; therefore, IE(H) and $IE(CH_3)$ are terms that are too large. This "overestimate" is "corrected for" by the methyl substituent effect on the protonation, $\Delta PA(CH_3)$. This term measures the relative energy stabilization of the ion due to some positive charge remaining on the H or CH_3.

As the proton affinity of the bases increases, $\Delta PA(CH_3)$ decreases, reaching a small value of a few kcal/mol (see plot of $\Delta PA(CH_3)$ in Figure 10A. This is expected because strongly basic groups (e.g., B = amine) will carry nearly all the positive charge and thus the relative charge remaining on the H or CH_3 is not so significant. The very small change of $\Delta PA(CH_3)$ at high PA values is responsible for the near linear region of the PA versus MCA plot in Figure 9, because when $\Delta PA(CH_3)$ becomes constant, PA(HX) and MCA(HX) become linearly related, (see eq 18).

A replot of the PA(B) and the MCA(B) data based on the functional dependence of eq 18 is shown in Figure 10B. The PA(B) – MCA(B) versus PA(B) plot illustrates the asymptotic approach to an approximately constant value at high PA(B) values. This asymptotic region corresponds to the linear region with slope $\rho = 1$ in the PA(B) versus MCA(B) plot in Figure 9.

Since the bond energy difference depends on the nature of the basic atom to which the bond is made, e.g., F, O, N, S, etc., somewhat different asymptotic values are expected for series of bases with a given basic atom. Thus, two high PA limits are observed in Figure 10b, the higher one corresponding to the nitrogen bases and the lower one to the sulfur bases. It will be interesting to see how the plot will look when MCA data for general bases B and not only for bases XH become available in the high affinity range.

e. Unique Features of Individual Methyl Cation Affinities. (i) Rare Gases. Methylated rare gas cations have previously been observed by Field et al.[32] as ions of very low abundance in electron impact studies of CH_4/rare gas mixtures at high pressures in a conventional mass spectrometer. However, the means of formation of these species was not identified nor were any data obtained
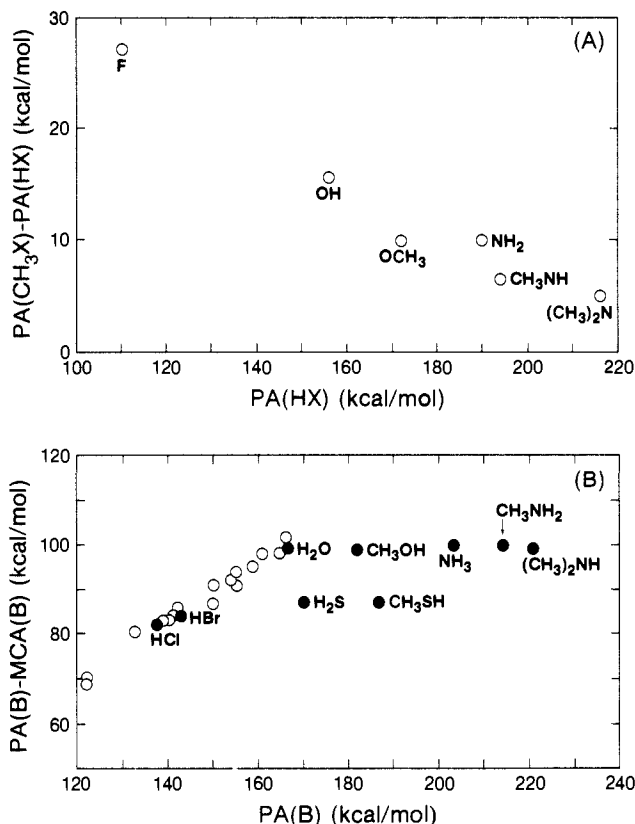

Figure 10. (A) Plot of $PA(CH_3X) - PA(HX)$ for X groups shown. (B) Plot of $PA(B) - MCA(B)$ versus $PA(B)$ reaches a constant value at high PA(B): (O) bases from Table III, (●) bases HX.

regarding their energetics. Reaction of Kr^+ with CH_4 at superthermal kinetic energies in a chemical accelerator study demonstrated the formation of CH_3Kr^+.[33] Based on ICR observations of methyl cation transfer equilibria, Hovey and McMahon[11,12] assigned methyl cation affinities of 51.5 ± 3 and 44.5 ± 3 kcal/mol for Xe and Kr, respectively.[34] Based on correlations of methyl cation affinity with proton affinity, it was further suggested that the methyl cation affinity of Ar should be $\sim$41 kcal/mol and might therefore be observable by CH_3^+ transfer from CH_3FH^+.

(ii) CO_2. Holmes et al.[35] have carried out collisional activation and metastable observation experiments on a variety of $C_2H_3O_2^+$ ions including CH_3OCO^+. In addition, ab initio calculations and appearance energy measurements were used to determine $\Delta H°_f(CH_3OCO^+)$. Based on an appearance energy of 11.24 eV for CH_3OCO^+ from $ClCO_2CH_3$ a value of $\Delta H°_f(CH_3OCO^+)$ of 126 kcal/mol was obtained corresponding to a methyl cation affinity of CO_2 of 41 kcal/mol. However, metastable peak observations indicated that formation of CH_3OCO^+ from $ClCO_2CH_3^+$ involves a significant reverse activation energy, establishing 41 kcal/mol as a lower limit to the methyl cation affinity of CO_2. Ab initio calculations yielded $\Delta H°_f(CH_3OCO^+)$ as 120 kcal/mol and a methyl cation affinity of CO_2 of 47 kcal/mol. However, the calculation did not involve a complete geometry optimization. Therefore, the value of 49.5 kcal/mol obtained in the present work appears to be quite reasonable and in agreement with the above results.

(iii) NF_3. Recent studies of protonation of NF_3 by both ion cyclotron resonance and ab initio techniques have demonstrated that the most favorable site of protonation of NF_3 is at fluorine

(32) Field, F. H.; Head, M. H.; Franklin, J. L. *J. Am. Chem. Soc.* 1962, *84*, 1118.

(33) Wyatt, J. R.; Stratten, L. W.; Hierl, P. M. *J. Phys. Chem.* 1976, *80*, 2911.

(34) The MCA values quoted[11,12] were higher by 3.5 kcal/mol. This was due to use of Beauchamp's[22a] $AP(CH_3N_2^+)$ in combination with an older and less reliable value for $\Delta H°_f(CH_3N_2CH_3)$.

(35) Blanchette, M. C.; Holmes, J. L.; Hop, C. E. C. A.; Lossing, F. P.; Postma, R.; Ruttink, P. J. A.; Terlow, J. K. *J. Am. Chem. Soc.* 1986, *108*, 7589.

rather than nitrogen.[36] As a result consideration must be given to possible methylation of NF_3 at both sites as well. A collision-induced decomposition experiment involving the $CH_3NF_3^+$ ion, derived from CH_4/NF_3 mixtures in the CI source of a reverse geometry double-focusing instrument, showed dominant loss of CH_3F to yield NF_2^+ and of NF_2H to yield CH_2F^+. These data are consistent with initial attachment of CH_3^+ to a fluorine of NF_3, eq 22. During the chemical activation process, an N–F bond

$$CH_3^+ + NF_3 \longrightarrow CH_3-\overset{+}{F}\diagdown_{N}\diagup^{-F}_{\diagdown F} \qquad (22)$$
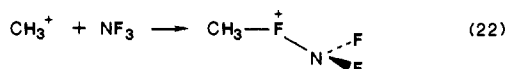
may be cleaved, leading directly to NF_2^+, or a tight ion–molecule complex may be formed ($CH_3F + NF_2^+$) from which NF_2^+ may insert in a C–H bond of CH_3F with subsequent unimolecular decomposition giving rise to $CH_2F^+ + NF_2H$. NF_2^+ has previously been shown[36] to readily insert into C–H bonds.

(iv) N_2O. N_2O is isoelectronic with CO_2 and has a greater basicity toward both H^+ and CH_3^+, and again the possibility of ambidentate character must be considered. In a high resolution infrared study of gaseous protonated N_2O, Amano[37] concluded that protonation takes place predominantly on oxygen. Collision-induced decomposition studies reveal evidence of both possible protonated forms of N_2O; however, CID of methylated N_2O was more strongly suggestive of methylation at nitrogen since the major fragmentation under CID conditions led to NO^+.[36]

(v) SO_2F_2 and SO_2. Both SO_2 and SO_2F_2 have frequently been used as solvents of low nucleophilicity in the study of superacids.[38] Gillespie has shown that solutions of $CH_3F/SbF_3,SO_2$ lead readily to formation of a new ionic species, CH_3OSO^+, which can be characterized by both NMR and X-ray crystallographic techniques.[39] Both Gillespie[40] and Olah[41] have demonstrated that

SO_2F_2 is a much more weakly coordinating solvent so that no $CH_3OSOF_2^+$ is formed, leaving only $CH_3^+SbF_6^-$ complexes in SO_2F_2 solution. This is in agreement with the present data which show SO_2 to bind CH_3^+ more strongly than SO_2F_2 by 5 kcal mol^{-1}. The comparable gas-phase basicities of SO_2F_2 and CH_3F toward CH_3^+ further suggest that under favorable conditions the dimethylfluoronium ion, $(CH_3)_2F^+$, might be observable by NMR. The present methyl cation affinity scale also provides useful suggestions for other potential solvents for "magic methyl" experiments.

(vi) OCS and CS_2. The similarity of the methyl cation affinities of COS and CS_2 and the larger difference between those of CO_2 and OCS suggest that OCS methylates at sulfur. The comparable methyl cation affinities of CS_2 and SO_2 also indicate that CS_2 might usefully be exploited as a solvent in superacid systems where it is desirable to work at temperatures above the liquid range of SO_2. To the best of our knowledge no such attempts have been made.

(vii) $(CF_3)_2CO$ and CF_3COCl. The trifluoromethyl group is known to significantly weaken the C=O bond as evidenced by the substantially lower stretching frequency for these carbonyls compared to that in $(CH_3)_2CO$. This leads to a reduced basicity of CF_3 substituted compounds relative to their pure hydrogenic analogues. This reduction in basicity and the slightly lower methyl cation affinity of CF_3COCl relative to CH_3Cl give rise to the possibility that CF_3COCl may, in fact, be a chlorine, rather than oxygen, base toward CH_3^+.

(36) Fisher, J. J.; McMahon, T. B. *J. Am. Chem. Soc.*, following paper in this issue.

(37) Amano, T. *Chem. Phys. Lett.* **1986**, *127*, 101. Amano, T. *Ibid.* **1986**, *130*, 154.

(38) Olah, G. A.; Surya Prakash, G. K.; Sommer, J. *Superacids*; Wiley: New York, 1985.

(39) Gillespie, R. J.; Riddel, F. G.; Slim, D. R. *J. Am. Chem. Soc.* **1976**, *98*, 8069.

(40) Calves, J. Y.; Gillespie, R. J. *J. Am. Chem. Soc.* **1977**, *99*, 1788.

(41) Olah, G. A.; Donovan, D. J. *J. Am. Chem. Soc.* **1978**, *100*, 5163.